SPECIAL
ISARS 2012
COLLECTION

A Twenty-First-Century California Observing Network for Monitoring Extreme Weather Events

A. B. WHITE,* M. L. ANDERSON,[+] M. D. DETTINGER,[#] F. M. RALPH,* A. HINOJOSA,[+] D. R. CAYAN,[#]
R. K. HARTMAN,[@] D. W. REYNOLDS,[&] L. E. JOHNSON,** T. L. SCHNEIDER,[++] R. CIFELLI,* Z. TOTH,*
S. I. GUTMAN,* C. W. KING,* F. GEHRKE,[+] P. E. JOHNSTON,[&] C. WALLS,[##] D. MANN,[##] D. J. GOTTAS,*
AND T. COLEMAN[&]

* NOAA/Earth System Research Laboratory, Boulder, Colorado
[+] California Department of Water Resources, Sacramento, California
[#] U.S. Geological Survey, and Scripps Institution of Oceanography, La Jolla, California
[@] NOAA/California Nevada River Forecast Center, Sacramento, California
[&] Cooperative Institute for Research in the Environmental Sciences, NOAA/University of Colorado Boulder,
and NOAA/Earth System Research Laboratory, Boulder, Colorado
** Cooperative Institute for Research in the Atmosphere, NOAA/Colorado State University, Fort Collins,
and NOAA/Earth System Research Laboratory, Boulder, Colorado
[++] NOAA/Office of Hydrologic Development, Boulder, Colorado
[##] UNAVCO, Inc., Boulder, Colorado

ABSTRACT

During Northern Hemisphere winters, the West Coast of North America is battered by extratropical storms. The impact of these storms is of paramount concern to California, where aging water supply and flood protection infrastructures are challenged by increased standards for urban flood protection, an unusually variable weather regime, and projections of climate change. Additionally, there are inherent conflicts between releasing water to provide flood protection and storing water to meet requirements for the water supply, water quality, hydropower generation, water temperature and flow for at-risk species, and recreation. To improve reservoir management and meet the increasing demands on water, improved forecasts of precipitation, especially during extreme events, are required. Here, the authors describe how California is addressing their most important and costliest environmental issue—water management—in part, by installing a state-of-the-art observing system to better track the area's most severe wintertime storms.

1. Introduction

Since the late 1990s, scientists from the National Oceanic and Atmospheric Administration (NOAA)'s Earth System Research Laboratory (ESRL) and their partners have been studying the winter storms that impact the U.S. West Coast each year. Beginning in 2004, this work was organized under the umbrella of NOAA's

Hydrometeorology Testbed (HMT-West; hmt.noaa. gov; Ralph et al. 2005; Morss and Ralph 2007). This paper describes a California HMT-Legacy project that has three main goals: 1) to install a twenty-first-century observing system to help address California's water and emergency management needs, 2) to provide a state-of-the-art numerical weather forecast model ensemble with a high-resolution nest over California, and 3) to develop decision support tools for weather and river forecasters and water managers. This project is part of the California Department of Water Resources (CA-DWR) Enhanced Flood Response and Emergency Preparedness Program.

The HMT-Legacy project is intended to help address some of the most extreme challenges that California faces regarding water and flood management in the face

Denotes Open Access content.

Corresponding author address: Dr. Allen B. White, NOAA/ Earth System Research Laboratory, R/PSD2, 325 Broadway, Boulder, CO 80305.
E-mail: allen.b.white@noaa.gov

of climate change. California's population and economies (including agriculture), and thus its demands for water, are expected to grow rapidly in coming decades, in a time when floods and storms are being projected to increase in magnitude and frequency (Das et al. 2011), when the state's snowpacks are expected to retreat and decline (Cayan et al. 2008, 2013), and when the state may face increasingly intense droughts.

The tension between increasing floods and decreasing snowpacks is tightly bound because California's reservoirs are used for both flood risk management and water supply purposes, with a volume of open space maintained for flood capture each winter that is nearly equal to the most optimistic projections of the volume of water that will no longer be stored in the state's snowpacks by midcentury under global warming (Knowles and Cayan 2004). The water that is not stored as snowpack most likely will run off in the winter months instead, often as flood flows. The projected earlier runoff thus is likely to become an important reason for keeping even more open space behind the state's dams (for even more flood control) but also corresponds to water that ideally could be saved until later in the year (behind those same dams) to meet growing warm-season urban, agricultural, and environmental demands (Cayan et al. 2010).

This dilemma facing reservoir managers is a paramount concern. If the future skill of week 1 and week 2 precipitation forecasts would be sufficient to be used in making water management decisions, this concern would be ameliorated. However, because there are no guarantees that sufficient forecast skill can be achieved, the HMT-Legacy project, in essence, is an insurance policy for California. The additional information about storms and floods and improvements in short-term (0–3 days) and perhaps even longer lead time forecasts that the new observations and numerical model ensemble may provide are of the utmost importance to the state's water and flood managers. Long-term operation of the observing network also will allow the state to track intraseasonal-to-decadal climate changes and better manage their consequences.

2. Selected scientific achievements from HMT-West

Following are some of the scientific achievements from HMT-West that motivated CA-DWR to invest in the HMT-Legacy project. A major finding from HMT-West is the role that atmospheric rivers (ARs), narrow regions of enhanced water vapor transported in the warm sectors of midlatitude cyclones, play in creating heavy precipitation that can lead to flooding (Ralph et al. 2004, 2006; Neiman et al. 2008; Guan et al. 2010; Lavers et al. 2011; Moore et al. 2012). As defined by

Ralph et al. 2004, ARs are long (>2000 km), relatively narrow (<1000 km), and concentrated (>2 cm of integrated water vapor) moisture plumes. Globally, ARs are a critical component of Earth's energy budget (Zhu and Newell 1998). In addition, climate projections suggest that the intensity and frequency of AR events in California may increase in response to global climate change (Dettinger 2011). An example of an AR impacting the U.S. West Coast as viewed from satellites (Wick et al. 2013) is shown in Fig. 1. The continents are black in Fig. 1 because the satellite microwave retrievals of water vapor that work over the oceans currently are not available over land, given the poorly known microwave emissivity of land surfaces (Prigent et al. 2000). In addition, satellites do not measure the winds in the low-level jet (Neiman et al. 2002) that focus the transport of moisture onshore and determine which watershed(s) will be impacted most by the AR (Ralph et al. 2003).

Water vapor is the fuel that generates precipitation, and Global Navigation Satellite Systems (GNSS) such as GPS offer a robust and reliable method of calculating vertically integrated water vapor (IWV; Bevis et al. 1992; Duan et al. 1996) with high temporal resolution under all weather conditions (Gutman et al. 2004). Also, unlike microwave satellite retrievals, GPS can provide accurate water vapor estimates over land. Peixoto and Oort (1992) showed that approximately 80% of the water vapor in the Northern Hemisphere atmosphere at midlatitudes exists in the lowest 700 mb, so IWV serves as a good proxy for the low-level moisture that fuels precipitation. For example, using four winters of IWV measurements collected on the northern coast of California, Neiman et al. (2009) showed that in order to produce $12 \, \text{mm h}^{-1}$ of rainfall in the coastal mountains, there needed to be at least 2 cm of IWV. This work helped to define the threshold of IWV that is now used to detect an AR.

In mountain watersheds, the altitude in the atmosphere where snow changes to rain (hereafter referred to as the snow level) can determine whether a storm augments the snowpack or creates a flood. White et al. (2002) used the National Weather Service (NWS) River Forecast System to simulate how changing the snow level would impact runoff in four California watersheds. For some of the watersheds they examined, a rise in the snow level of 600 m could more than triple the peak runoff in the watershed for the precipitation associated with a modest storm. Because of the importance of the snow level in mountain hydrology, White et al. (2010) began to evaluate the accuracy of snow-level forecasts produced by the NWS using snow-level observations collected with vertically pointing precipitation profilers (White et al. 2000) and found that significant forecast errors (300–900 m) occurred for some of the wettest storms.
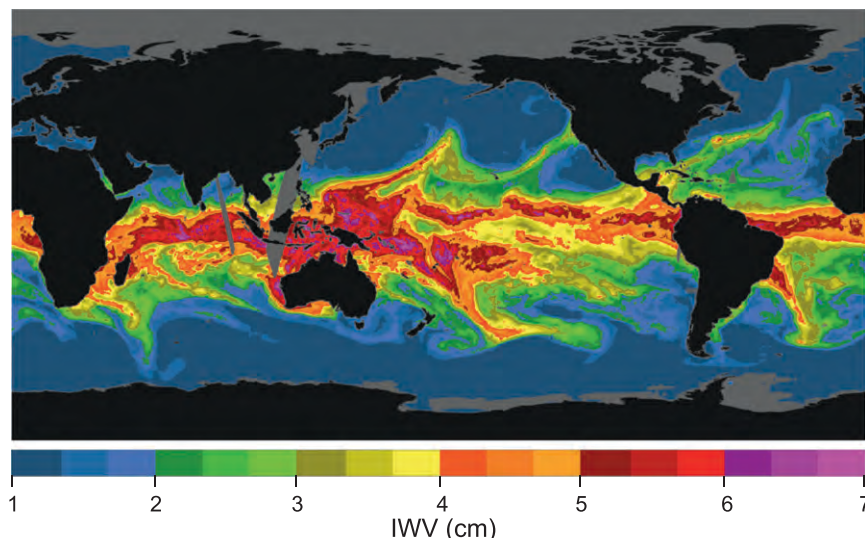
FIG. 1. Global composite satellite image of IWV (cm) measured with the Special Sensor Microwave Imager (SSM/I) aboard the Defense Meteorology Satellite Program constellation. The image is composited from satellite overpasses that occurred during the post meridiem hours (UTC) of 16 Feb 2004. Several narrow AR corridors are noticeable in the midlatitudes, including one that is impacting the U.S. West Coast.

The timing of a storm within the winter wet season can also determine whether a flood will ensue. For early season storms the antecedent soil conditions are normally dry, such that much of the precipitation is absorbed by the ground, thereby minimizing runoff. Later in the wet season, the timing between subsequent storms determines whether the soils dry out sufficiently to absorb some or all of the rainfall from the next precipitation event (Zamora et al. 2011). An example indicating the streamflow response to soil moisture conditions in the Russian River watershed in Sonoma County, California, is shown in Fig. 2. The watershed was impacted by three separate precipitation events within a 5-day period from late November through early December 2012. Peaks in the Russian River streamflow were observed each time the observed precipitation rate and amount kept the 10-cm soil at field capacity for a period longer than 3 hours. The $424.8 \, m^3 \, s^{-1}$ (15 000 cfs) flow peak occurred early on 3 December after the soil at 15-cm depth exceeded the field capacity by 14% volumetric water content, as a result of the saturation–excess runoff (Dunne and Black 1970). The maximum flow stage corresponding to this peak streamflow was 5.98 m, which is 0.42 m below flood stage for this particular location on the Russian River.

3. A tiered approach to observing system enhancements

All of the aforementioned findings from HMT-West influenced the design of the observing network that

ESRL proposed to CA-DWR in 2007. The basic strategy was to organize different observing projects in a series of successive tiers, forming a pyramid. Each tier incorporates and builds on the previous tier(s) by adding new projects with increased scope, complexity, and/or cost. For example, tier 1 involves networks of sensors that have a proven track record and are relatively inexpensive to acquire, deploy, operate, and maintain. This tier consists of precipitation gauges, soil moisture probes, integrated water vapor sensors using existing GPS/GNSS receivers, and a new snow-level radar (Johnston et al. 2012) that was designed specifically for the HMT-Legacy project. Tier 1 also takes advantage of existing observing infrastructure within California. For example, NOAA is partnering with the University NAVSTAR Consortium (UNAVCO; www.unavco.org)[1] to upgrade existing GPS receivers across California with meteorological measurements and real-time communications to allow for continuous retrievals of IWV.

Tier 2 consists of observing technology that is mature but that comes at a higher cost than observing technology in tier 1. Given the importance of ARs in generating heavy precipitation and floods and the gaps associated with satellite remote sensing, ESRL scientists had previously designed, deployed, and tested a combination of

---

[1] Operators of the PBO, the geodetic component of EarthScope funded by the National Science Foundation.
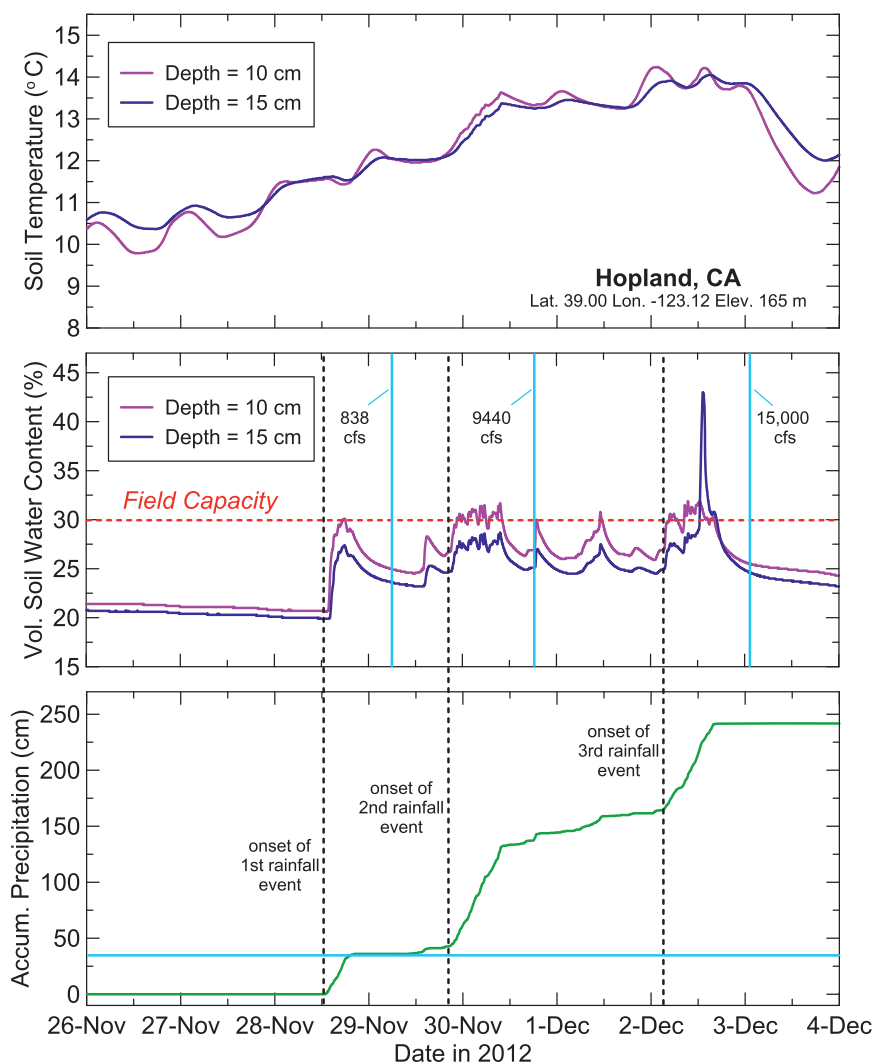
FIG. 2. (top) Soil temperature (°C), (middle) volumetric soil water content (%), and (bottom) accumulated precipitation (cm) observed at the HMT-Legacy project site at Hopland, California, from 0000 UTC 26 Nov 2012 to 1400 UTC 3 Dec 2012. Peaks in Russian River streamflow provided by the U.S. Geological Survey (USGS) are indicated by blue vertical lines in the middle panel. The thin horizontal line in the bottom panel indicates the amount of rainfall that was required to achieve field capacity initially for the 10-cm soil moisture probe.

sensors, called an atmospheric river observatory (ARO; White et al. 2009, section 4d), that could detect and monitor the important physical parameters of ARs as they make landfall. A statewide network of AROs was proposed to CA-DWR under tier 2.

The upper tiers (3 and 4) have observing projects that may not have been fully evaluated in the research community and/or are significantly more expensive to implement than the observing projects in tiers 1 and 2. Examples include buoy-mounted wind profilers (Jordan et al. 1998), gap-filling radars (Matrosov et al. 2005; Jorgensen et al. 2011), and a Pacific winter storms

reconnaissance program akin to the hurricane reconnaissance program conducted each year over the Atlantic Ocean. These ideas are scientifically tractable, and NOAA has made progress in each of these areas over the past several years. For example, NOAA, the National Center for Atmospheric Research (NCAR), and the National Aeronautics and Space Administration (NASA) used a new automated dropsonde system on an unmanned aircraft to study atmospheric rivers over the Pacific Ocean in February 2011 for a project called Winter Storms and Pacific Atmospheric Rivers (WISPAR). ESRL is also collaborating with the NWS
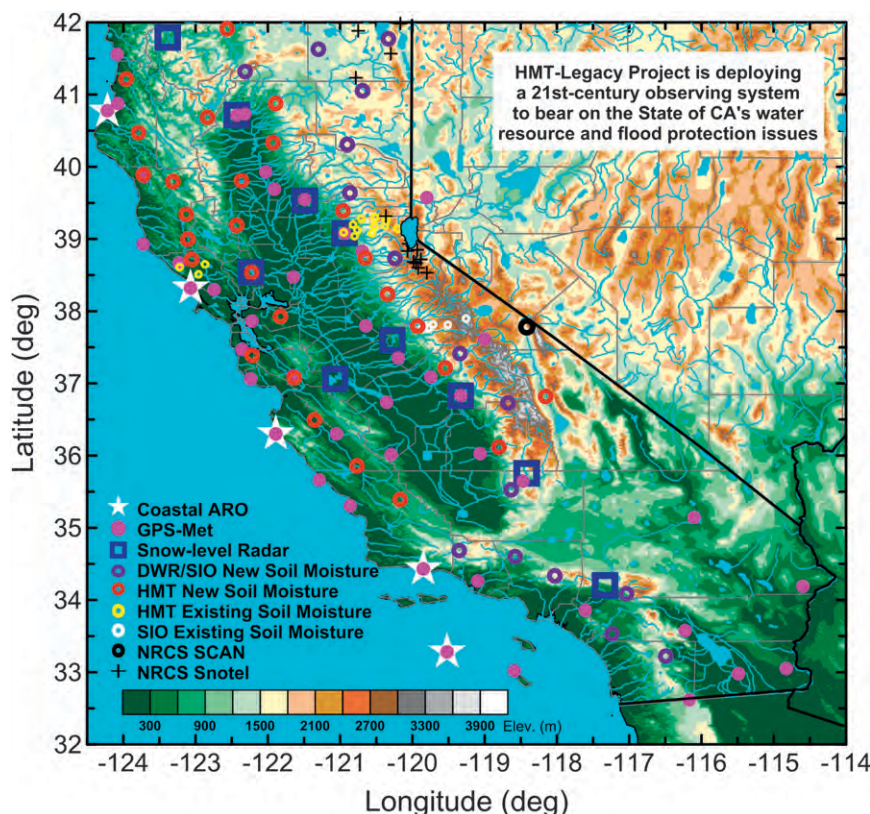
FIG. 3. Map of California indicating where the four observing system enhancement projects are being implemented as part of the HMT-Legacy project.

and NOAA's National Severe Storms Laboratory to evaluate the benefit of gap-filling radar to improve quantitative precipitation estimation in an area of California that has particularly poor coverage from the NWS operational radar network Next Generation Weather Radar (NEXRAD). This project is in conjunction with the Sonoma County Water Agency and the San Francisco CBS television network affiliate, KPIX, who installed a Doppler weather radar on Mount Vaca in Napa and Solano Counties, based largely on HMT's prior demonstration of gap-filling radar on the Sonoma County coast (Matrosov et al. 2005). A similar method of tiers (not discussed) was used to propose projects involving numerical modeling, information display, and decision support.

The original agreement signed with CA-DWR in 2008 was to implement the observing, numerical modeling, display, and decision support projects from tier 1. The Scripps Institution of Oceanography (SIO) is a coinvestigator on the observing implementation plan. In 2010, CA-DWR amended the agreement to include a coastal network of four AROs from tier 2. Figure 3 shows a map of where each of the observing networks is being deployed. A follow-on agreement will define how

the observing networks will be operated and maintained after 2013.

4. Observing system and forecast model descriptions

a. Soil probes and surface meteorological sensors

The HMT-Legacy project calls for the installation of 43 integrated soil moisture, soil temperature, and surface meteorology stations. ESRL is responsible for installing 27 of the 43 stations. ESRL decided to partner with the California Department of Forestry and Fire Protection (CAL FIRE) for the bulk of these installations because the numerous CAL FIRE station locations offered a variety of soil and meteorological conditions, site access was easy, and site security is more than adequate. In addition, the CAL FIRE station staff appreciate having access to the local surface meteorological data that are being provided as part of this project to help portray fire weather conditions during the dry season. Table 1 lists the instruments comprising the ESRL installations. Initially, soil probes are being installed at two depths at each site: 10 and 15 cm. Some of the soil probe

TABLE 1. Instruments deployed in the HMT-Legacy soil-probe and surface meteorology sensor network stations installed by ESRL.

Variable	Instrument	Type	Accuracy
Air temperature	Campbell Scientific CS215	Sensirion SHT 75 Single chip element	± 0.3°C at 25°C ± 0.4°C from $+5$° to $+40$°C
Relative humidity	Campbell Scientific CS215	Sensirion SHT75 Single chip element	$\pm 2\%$ from 10% to 90% $\pm 4\%$ from 0% to 100%
Precipitation	Texas Electronics TR-525I	Tipping bucket	$\pm 1\%$ up to 0.254 mm h^{-1} 0%–3% from 25.4 to 50.8 mm h^{-1} 0%–5% from 50.8 to 76.2 mm h^{-1}
Soil temperature	Campbell Scientific T107	Thermistor	± 0.4°C in worst case
Soil wetness	Campbell Scientific CS616	Reflectometer	$\pm 2\%$

installations in key watersheds will receive or will be retrofitted with additional probe depths that are consistent with both the U.S. Department of Agriculture (USDA) Natural Resources Conservation Service (NRCS) Soil Climate Analysis Network (SCAN) and the U.S. Climate Reference Network (USCRN) probe depths (5, 10, 20, 50, and 100 cm). The soil probe and meteorological sensor signals are acquired through a Campbell Scientific, Inc. CR800 datalogger. Soil and surface

meteorology data (2-min averages) are transmitted once every hour to a data hub in Boulder, Colorado, through one of three communication methods: telephone, satellite, or cellular services. Figure 4 shows a typical ESRL soil probe and surface meteorology installation in the HMT-Legacy network.

CA-DWR and SIO are jointly responsible for installing the remaining 16 soil/surface meteorology stations. Because many of these stations were intended to
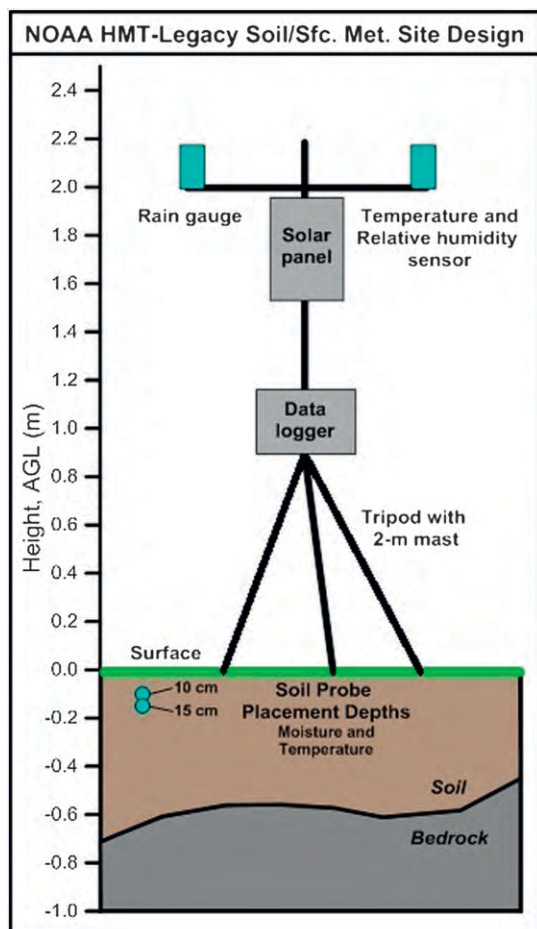

FIG. 4. (left) Schematic of the ESRL soil probe and surface meteorology sensor site design and (right) the actual HMT-Legacy project network deployment at O'Neals, California.

TABLE 2. Instruments deployed in the HMT-Legacy soil-probe and surface meteorology sensor network stations installed by CA-DWR/SIO. In the "Type" and "Accuracy" columns, the sensors and data communications supported by RAWS interagency partners can be found online (http://raws.fam.nwcg.gov/stationassets.html).

Variable	Instrument	Type	Accuracy
Air temperature	Various	RAWS	RAWS
Relative humidity	Various	RAWS	RAWS
Station pressure	Various	RAWS	RAWS
Wind speed	Various	RAWS	RAWS
Wind direction	Various	RAWS	RAWS
Precipitation	Various	RAWS	RAWS
Soil temperature	Campbell Scientific T107	Thermistor	$\pm0.4°C$ in worst case
Soil wetness	Campbell Scientific CS616	Reflectometer	$\pm2\%$

be at higher elevations, it was both efficient and cost effective to take advantage of the existing infrastructure available at the Remote Automated Weather Station (RAWS) network run by the U.S. Forest Service and Bureau of Land Management and monitored by the National Interagency Fire Center. Table 2 lists the soil-probing and surface meteorology instruments comprising the CA-DWR/SIO installations. The installation depths are 5, 10, 20, and 50 cm. Because of the soil structure, not all depths will be populated at all installation sites. Table 3 lists the site locations where NOAA and CA-DWR/SIO are installing soil and surface meteorology equipment for the HMT-Legacy project.

b. GPS integrated water vapor

Hundreds of continuously operating GPS receivers have been installed in California primarily for surveying and geodetic science purposes. Outfitting a GPS receiver site with temperature and pressure measurements allows real-time retrieval of the IWV. We will refer to GPS receiver sites with this configuration as GPS-Met sites, which is also the name of the program in NOAA that provides IWV estimates retrieved from GNSS signal delays to NOAA weather forecasters, NOAA weather forecast models, and researchers around the world. Many of the existing GPS receiver sites in California are part of the National Science Foundation's Plate Boundary Observatory (PBO) that is operated by UNAVCO.

The HMT-Legacy project calls for 36 GPS-Met sites to provide estimates of IWV throughout California. Some of these sites were only equipped with GPS receivers and are being retrofitted by UNAVCO with the necessary meteorological sensors. Others are existing GPS receiver sites in the PBO network that were already GPS-Met compatible but needed real-time communications to make them useful for operational weather forecasting applications. Because of the initial success of the project, UNAVCO has added six additional GPS-Met sites to the California network to support this application in areas

devoid of atmospheric or geodetic observations. Finally, some of the GPS-Met sites are collocated with other new or existing HMT-West observing sites in this project, particularly where it made scientific sense to have IWV measurements available with another type of atmospheric measurement. Table 4 lists the new GPS-Met sites that were made available as part of the HMT-Legacy project.

The GPS receiver signals and surface meteorological data from the GPS-Met stations are transmitted to Boulder via the internet, where they are combined with continuously updated GPS satellite orbit information provided by the Scripps Orbit and Permanent Array Center at the University of California San Diego to calculate IWV in near-real time. Currently IWV is estimated every 30 minutes for numerical weather prediction and satellite calibration/validation purposes. However, an experiment underway in 2013 is examining whether shorter (5–15 min) averaging periods can provide accurate estimates of IWV that are useful to forecasters during rapidly changing extreme weather conditions associated with ARs, the North American monsoon, and Santa Anna conditions. Estimates of IWV from the HMT-Legacy GPS-Met network are available on NOAA's GPS-Met home page (http://gpsmet.noaa.gov/). Values of IWV are also combined with satellite observations to provide a blended IWV product that is available from the Cooperative Institute for Research in the Atmosphere (http://amsu.cira.colostate.edu/gpstpw/) and the National Centers of Environmental Prediction (NCEP; http://www.osdpd.noaa.gov/bTPW/).

c. Snow-level radars

The pulsed Doppler radars that have been used in HMT-West to provide measurements of the snow level during precipitation are relatively expensive to acquire, transport, deploy, operate, and maintain. One of the goals of the HMT-Legacy project was to develop a less expensive instrument that would be easier to transport, deploy, operate, and maintain. Radar engineers at ESRL

TABLE 3. Locations of the soil-probe and surface meteorological sensor station installations in the HMT-Legacy project. TBD indicates to be determined.

Location	Station ID	Lat (°)	Lon (°)	Elev (m)	Installation by	Installation date
Hornbrook, CA	HBK	41.904	−122.569	715	ESRL	13 Sep 2011
Cold Springs, CA	CSZC1	41.781	−120.319	1944	CA-DWR/SIO	TBD
Timber Mountain, CA	TBRC1	41.628	−121.298	1540	CA-DWR/SIO	TBD
Mt. Shasta, CA	MSAC1	41.315	−122.317	1089	CA-DWR/SIO	TBD
Orick, CA	ORK	41.223	−124.054	392	ESRL	TBD
Ash Valley, CA	AVLC1	41.052	−120.686	1554	CA-DWR/SIO	TBD
Montgomery Creek, CA	MGC	40.867	−121.886	1051	ESRL	TBD
Weaverville, CA	WVV	40.677	−122.831	643	ESRL	TBD
Bridgeville, CA	BGV	40.474	−123.793	215	ESRL	TBD
Paynes Creek, CA	PCK	40.333	−121.924	563	ESRL	TBD
Lassen County, CA	WWDC1	40.306	−120.903	1876	CA-DWR/SIO	TBD
Leggett, CA	LEG	39.876	−123.720	280	ESRL	TBD
Black Butte Lake, CA	BBL	39.813	−122.369	160	ESRL	14 Nov 2012
Saddleback, CA	SLEC1	39.638	−120.865	2033	CA-DWR/SIO	TBD
Nevada City, CA	NVC	39.385	−120.978	1055	ESRL	19 Apr 2011
Willits, CA	WLS	39.346	−123.317	594	ESRL	17 Dec 2010
Potter Valley, CA	PTV	39.336	−123.138	303	ESRL	20 Apr 2011
Leesville, CA	LVE	39.184	−122.436	436	ESRL	TBD
Hopland, CA	HLD	39.003	−123.121	164	ESRL	10 May 2011
Owens Camp, CA	OWNC1	38.736	−120.242	1597	CA-DWR/SIO	TBD
Camino, CA	CMN	38.735	−120.664	1003	ESRL	30 Mar 2011
Lake Sonoma, CA	LSN	38.719	−123.054	396	ESRL	17 Dec 2010
Lake Berryessa, CA	LBY	38.539	−122.234	204	ESRL	TBD
Arnold, CA	AND	38.235	−120.364	1176	ESRL	18 Apr 2011
Clayton, CA	CTN	37.899	−121.860	191	ESRL	TBD
Hodgdon Meadow, CA	HDM	37.796	−119.859	1397	ESRL	24 Jun 2010
Minarets, CA	MTTC1	37.407	−119.346	1619	CA-DWR/SIO	TBD
Los Gatos, CA	LGS	37.262	−122.133	786	ESRL	TBD
O'Neals, CA	ONS	37.204	−119.570	684	ESRL	29 Mar 2011
Gilroy, CA	GRY	37.072	−121.479	273	ESRL	TBD
Independence, CA	IDP	36.799	−118.195	1198	ESRL	TBD
Park Ridge, CA	PRGC1	36.724	−118.943	2298	CA-DWR/SIO	TBD
Soledad, CA	SLD	36.461	−121.381	53	ESRL	TBD
Springville, CA	SPV	36.192	−118.802	450	ESRL	TBD
Lockwood, CA	LWD	35.937	−121.108	312	ESRL	TBD
Democrat, CA	DEMC1	35.532	−118.631	721	CA-DWR/SIO	9 Jan 2013
Santa Margarita, CA	SMG	35.381	−120.189	501	ESRL	TBD
Ozena, CA	OZNC1	34.682	−119.354	1125	CA-DWR/SIO	10 Jan 2013
Warm Springs, CA	WMSC1	34.596	−118.579	1503	CA-DWR/SIO	TBD
Chilao, CA	CHOC1	34.332	−118.030	1661	CA-DWR/SIO	TBD
Beaumont, CA	BNTC1	33.931	−116.950	794	CA-DWR/SIO	TBD
Santa Rosa Plateau, CA	SRUC1	33.518	−117.229	606	CA-DWR/SIO	TBD
Julian, CA	JULC1	33.076	−116.593	1292	CA-DWR/SIO	TBD

and the University of Colorado's Cooperative Institute for Research in the Environmental Sciences designed and prototyped a new frequency modulated–continuous wave (FM–CW) radar operating at 10-cm wavelength for this project (Johnston et al. 2012).

Instead of transmitting a pulsed signal, the FM–CW radar transmits continuously, which requires separate antennas to transmit and receive so the transmitter does not saturate the receiver. The range of the targets is determined by changing the transmitted frequency during the observations. When the echoes are received, the

frequency is measured and converted into range. Constant transmission also allows the radars to be low powered, which simplifies the radar electronics and allows the design to take advantage of readily available components. In production mode, the parts to build one of these new FM–CM radars would be about an order of magnitude less expensive than the parts required to build a higher-powered pulsed radar designed for the same purpose.

These small "snow-level radars" (Fig. 5) use two vertically pointed 1.2-m-diameter parabolic reflectors

TABLE 4. Locations of the GPS-Met stations in the HMT-Legacy project.

Location	ESRL station ID	Lat (°)	Lon (°)	Elev (m)	Collocated with other HMT equipment or PBO site ID	Providing IWV data since
Klamath, CA	KLM	41.559	−124.086	235	P316	7 Nov 2011
McKinleyville, CA	ACV	40.972	−124.110	58	Wind profiler	TBD
Humboldt, CA*	HMB	40.876	−124.075	21	P058	22 Jun 2012
Wonderland, CA*	WDL	40.731	−122.319	275	P349	22 Jun 2012
Shasta Dam, CA	STD	40.716	−122.429	206	Snow-level radar	9 Dec 2009
Corning, CA	CRN	39.929	−122.028	50	P344	7 Nov 2011
Leggett, CA	LGT	39.864	−123.717	258	P315	7 Nov 2011
Chico, CA*	CCO	39.700	−121.908	42	Wind profiler	19 Jun 2000
Reno, NV	DRN	39.573	−119.800	1504	P090	3 Dec 2009
Oroville, CA	OVL	39.532	−121.488	114	Snow-level radar	7 Nov 2011
Colfax, CA	CFC	39.079	−120.938	644	Wind profiler	13 Nov 2007
Point Arena, CA	PAN	38.928	−123.726	21	P059	3 Dec 2009
Placerville, CA	SMT	38.829	−120.693	1079	P140	3 Dec 2009
Annapolis, CA	BRG	38.668	−123.230	209	P188	3 Dec 2009
Dixon, CA	FFM	38.474	−121.646	7	P268	3 Dec 2009
Bodega Bay, CA	BBY	38.319	−123.073	16	Wind profiler	5 Apr 2013
Petaluma, CA	MHL	38.298	−122.743	91	P196	3 Dec 2009
Berkeley, CA	SVC	37.864	−122.219	407	P224	3 Dec 2009
Oakdale, CA	WCC	37.795	−120.644	83	P306	3 Dec 2009
Mammoth Lakes, CA	OMM	37.613	−119.000	2741	P630	3 Dec 2009
Redwood City, CA	MCK	37.472	−122.357	434	P176	3 Dec 2009
Planada, CA	PLD	37.352	−120.197	96	P305	3 Dec 2009
Morgan Hill, CA	LCD	37.104	−121.651	72	P217	3 Dec 2009
Coarsegold, CA	SER	37.089	−119.746	332	P725	10 Dec 2010
Davenport, CA	CPK	37.061	−122.238	205	P534	3 Dec 2009
Pine Flat Dam, CA	PFD	36.830	−119.332	184	Snow-level radar	6 Dec 2010
Mendota, CA	MTA	36.739	−120.357	17	P304	10 Dec 2010
Point Sur, CA	PTS	36.304	−121.888	13	Wind profiler	TBD
King City, CA	LOG	36.302	−121.051	343	P174	10 Dec 2010
Potterville, CA	PRV	36.027	−119.063	102	P056	10 Dec 2010
Coalinga, CA	CCY	36.016	−120.294	324	P298	10 Dec 2010
Kernville, CA	KNV	35.754	−118.419	816	Snow-level radar	25 Apr 2012
Point Piedras Blancas, CA*	PPB	35.666	−121.285	10	Wind profiler	3 Jan 2005
Los Osos, CA	LSO	35.304	−120.860	41	P523	10 Dec 2010
Baker, CA	BKR	35.142	−116.104	263	P618	7 Nov 2011
Goleta, CA	GLA	34.429	−119.847	3	Wind profiler	TBD
Somis, CA	SMS	34.263	−119.096	37	P729	7 Nov 2011
Vidal Junction, CA*	VDJ	34.189	−114.599	268	P623	22 Jun 2012
Corona, CA	CNA	33.858	−117.609	300	CNPP	29 Nov 2011
La Quinta, CA	LQT	33.575	−116.227	4	P491	7 Nov 2011
San Nicolas Island, CA	SNS	33.280	−119.522	16	Wind profiler	23 Jun 2010
Glamis, CA*	GMP	33.051	−114.827	591	CMPK	22 Jun 2012
Brawley, CA*	DSC	32.980	−115.488	74	P499	22 Jun 2012
San Clemente Island, CA*	SCL	32.914	−118.488	491	GPS-Met only	TBD
Jacumba, CA*	JCB	32.617	−116.17	823	P066	22 Jun 2012

* A site run by NOAA or UNAVCO, Inc. that is not included in the HMT-Legacy agreement.

for antennas. The antennas are enclosed in shrouds that have steep covered openings so that snow can slide off and not impact operation of the radar. These antennas have asymmetrical side lobes that allow the radars to be situated at sites that otherwise would produce ground clutter for other types of vertically pointing radars. The electronics for the snow-level radar are located in the narrow compartment between the antennas. The compartment is insulated and has a heater and air conditioner. This allows the radar to be all-weather capable, while using commercial-grade computers and electronics. The entire radar is mounted on a flat 4.5-m-long utility trailer so it can be easily transported, positioned, and leveled, although the installations for the HMT-Legacy project are intended to be permanent. Table 5 lists the engineering characteristics of the snow-level radar. Table 6 lists the locations of the 10 snow-level radars that are being installed near major reservoirs across California for the HMT-Legacy project.

FIG. 5. (right) The snow-level radar, (middle) surface meteorological sensors, and (left) GPS receiver antenna deployed at Pine Flat Dam, California, for the HMT-Legacy project. The 1.2-m diameter radar transmit and receive antennas are placed at the bottom of the sloped antenna enclosures wrapped in marine cover plastic. The sloped covers help shed snow and/or pooling water, which would otherwise inhibit radar performance. The radar electronics and data acquisition computer are situated inside the environmentally controlled cabinet placed between the two antenna enclosures.

During precipitation, an automated algorithm based on White et al. (2002) analyzes profiles of radar reflectivity and Doppler vertical velocity measured by the snow-level radar to determine if a radar brightband (Battan 1959) is present. If a brightband exists, the algorithm chooses the peak radar reflectivity in the brightband to represent the snow level. The algorithm is applied to 10-min blocks of radar data and the results are transmitted hourly to the data hub in Boulder, Colorado, via one of the three communication services described earlier. An example of the real-time snow-level product display derived from a snow-level radar in the HMT-Legacy project is shown in Fig. 6. If a brightband is not detected, the time–height cross section of Doppler vertical velocity is still displayed.

d. Atmospheric river observatories

The original ARO concept (White et al. 2009) consisted of an observation couplet: one site at the coast instrumented with a Doppler wind profiler (Carter et al. 1995) to measure the incoming airflow profile and a GPS-Met station to measure the IWV and surface meteorology and a second site downwind in the coastal mountains instrumented with an S-band precipitation profiling radar (White et al. 2000), disdrometer, and surface meteorology to characterize the bulk microphysics of the orographically enhanced rainfall (White et al. 2003; Neiman et al. 2005; Kingsmill et al. 2006; Martner et al. 2008), as well as the orographic precipitation enhancement ratio. Measuring the wind profile is critical because the winds in the low-level jet are most highly correlated with the orographically enhanced rainfall, while the winds near the surface can often be blocked by the terrain (Neiman et al. 2002). Combining the winds in the low-level jet with the measured IWV, used as a proxy for the low-level moisture, allows the calculation of the bulk flux of water vapor, which Neiman et al. (2009) showed to be more highly correlated with orographic rainfall than either the winds in the low-level jet core or the IWV, treated separately. Figure 7 illustrates the scientific concepts behind the ARO development.

Where possible, given noise considerations, the AROs will include a Radio Acoustic Sounding System (RASS) for temperature profiling (Moran and Strauch 1994). The RASS is particularly useful for characterizing the atmospheric stability in AR conditions and is also useful for measuring the depth and strength of the marine inversion, which is often prevalent along the coast during the dry season. Table 7 lists the engineering specifications for the 449-MHz wind profiler with RASS, the particular wind profiler technology chosen for the AROs in this project based largely on a yearlong wind profiler technology evaluation conducted by ESRL from September 2005 to August 2006 (see http://www.esrl.noaa.gov/psd/psd2/programs/ioos/). Figure 8 shows the ARO installed on San Nicolas Island off the coast of Southern California. This particular installation is

TABLE 5. Characteristics of the newly developed snow-level radar for the HMT-Legacy project.

Parameter	Unit	Typical configuration	Min value	Max value
Frequency	GHz	2.835	2.835	2.835
Antenna diameter	m	1.2	1.2	1.2
Average transmit power	W	0.7	0.6	12
Beamwidth	°	5.7	5.7	5.7
Range resolution (-3 dB response)	m	46.4	15.1	116
Range gate spacing	m	40	13	100
Snow-level determination period	min	10	5	60
Nyquist velocity	m s^{-1}	21.5	10.0	24.0
Number of spectral points	No.	256	64	1024
Number of heights	No.	252	1	512
Lowest height	m (above radar)	20	10	100
Highest observed height	m (above radar)	10 060	6000	51 000

TABLE 6. Locations of the snow-level radars being installed for the HMT-Legacy project. All are installed by ESRL.

Location	Station ID	Lat (°)	Lon (°)	Elev (m)	Installation date
Happy Camp, CA	HCP	41.791	−123.385	368	7 Nov 2011
Shasta Dam, CA	STD	40.716	−122.429	206	9 Dec 2009
Oroville, CA	OVL	39.532	−121.488	114	7 Nov 2011
Colfax, CA	CFC	39.079	−120.938	644	13 Nov 2007
Lake Berryessa, CA	LBY	38.539	−122.233	205	TBD
New Exchequer Dam, CA	NER	37.597	−120.277	259	3 Dec 2010
San Luis Reservoir, CA	SLR	37.061	−121.067	81	2 Apr 2013
Pine Flat Dam, CA	PFD	36.830	−119.332	184	6 Dec 2010
Kernville, CA	KNV	35.754	−118.419	816	25 Apr 2012
San Bernardino, CA	SBO	34.203	−117.335	600	12 Mar 2013

supported by the U.S. Navy, but the same technology and setup will be used for the four coastal AROs supported by the HMT-Legacy project.

For the HMT-Legacy project, CA-DWR gave priority to installing a "picket fence" of single-site AROs along the coast rather than investing in fewer AROs and using saved resources to support the observing couplets, as in the original ARO concept. ESRL has operated an ARO couplet in Sonoma County, California, as part of the HMT-West since the winter of 1997/98. They plan to continue operating this particular ARO couplet during each upcoming winter wet season for as long as possible to gather more insight into the orographic processes working at relatively short distances (~10 km) from the coast and to provide long-term observations of ARs making landfall in an important agricultural and ecological region. Table 8 lists the locations of the four AROs that are being installed for the HMT-Legacy project. These specific locations were chosen to form an ARO picket fence, as CA-DWR desired, but they were

also places where ESRL had experience successfully operating an ARO in the past for a variety of projects related to HMT-West.

e. Data ingest and display

ASCII data files and display graphics from the observing networks are generated within minutes after being received at the data hub and are made publicly available online (http://www.esrl.noaa.gov/psd/data/obs/). Data are also distributed through NOAA's Meteorological Assimilation Data Ingest System (MADIS; http://madis.noaa.gov/), the California Data Exchange Center (CDEC; http://cdec.water.ca.gov/), and are distributed in a specialized NWS data format to NWS Weather Forecast Offices (WFOs) and the California Nevada River Forecast Center (CNRFC) through NWS Western Region Headquarters.

Data from the HMT-Legacy project observing networks are also being displayed in Google Maps, as in Fig. 9. This display mimics the type of observational
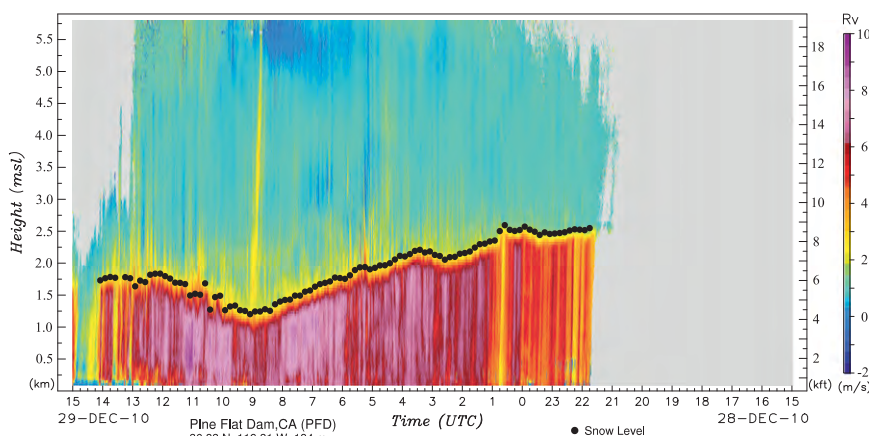

FIG. 6. Example snow-level product display from 1500 UTC 28 Dec 2010 to 1500 UTC 29 Dec 2010 measured by the snow-level radar deployed at Pine Flat Dam, California, for the HMT-Legacy project. The color contours indicate the Doppler velocity (m s^{-1}; positive downward; scale to the right) measured by the radar, which is dominated in precipitation by the fall speed of the hydrometeors (snow crystals or rain drops). The snow level is indicated by black dots. The images are updated hourly and are publicly available online.
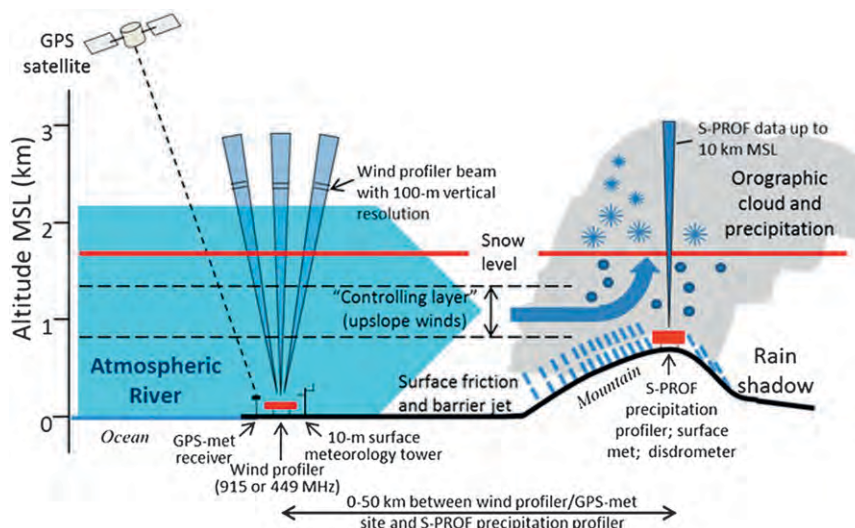
FIG. 7. Schematic of the coastal ARO-observing couplet. The controlling layer winds are where the highest correlation exists between the upslope component of the flow (perpendicular to the terrain) and the orographically enhanced rainfall observed at the mountain site. The HMT-Legacy project AROs will not have the instruments shown here at the mountain site. However, the NWS and cooperative agencies operate rain gauges in the mountains upstream from all of the planned ARO locations.

displays used by NWS field offices. Currently the following near-real-time surface meteorology measurements are available in this display: temperature, integrated water vapor, snow depth, wind speed, wind direction, and accumulated precipitation for the past 1-, 3-, 6-, 12-, or 24-h periods. In addition, the following remotely sensed data products are available: snow level, integrated water vapor flux, NEXRAD reflectivity mosaic, and NEXRAD 1-h precipitation mosaic. Time series displays of these and other HMT-West datasets, excluding the NEXRAD products, are available through the product availability table (http://www.esrl.noaa.gov/psd/data/obs/). A similar Google Maps display tool is available to view instrument inventories and to see where different types of ESRL instruments have been deployed for HMT-West and other field projects (http://www.esrl.noaa.gov/psd/data/obs/sitemap/psdmapsite.data.php).

f. The HMT weather forecast model

To take full advantage of the observing networks being installed and to provide advanced lead time for high-impact weather events, the HMT-Legacy project includes a data assimilation and numerical weather prediction system. The weather forecast model is the most current release (v3.4.1) of the Weather Research and Forecasting (WRF) model (Skamarock and Klemp 2008). The configuration employed for the HMT-Legacy project uses the Advanced Research WRF (ARW) dynamic core. An eight-member ensemble covering North America (beginning in 2013) is run at 9-km grid spacing with 35 vertical levels. A variety of initial and boundary conditions, as well as physical parameterizations, are used to differentiate the ensemble members. Initial conditions are provided by blending the Global Forecast System (GFS) with local observations using the Local Analysis and Prediction System (LAPS; Albers et al. 1996; Toth et al. 2012). Lateral boundary conditions are updated

TABLE 7. Characteristics of the 449-MHz wind profiler and RASS that are part of the AROs being deployed for the HMT-Legacy project.

Wind profiler	Unit	Typical configuration
Frequency	MHz	449
Antenna type	—	Coaxial–colinear phased array
Antenna diameter	m	6
Beamwidth	°	10
Peak transmit power	W	2000
Transmit pulse width	μs	0.708, 2.833
Height coverage	m	180–8000
Range gate spacing	m	106, 212
Temporal resolution	min	60
RASS		
Frequency	kHz	Random sweep around 1.0
Number of source/ receive antennas	No.	4
Acoustic power	dB	60 dB at 30 m above antenna
Height coverage	m	1500–2000
Range gate spacing	m	106

FIG. 8. The ARO installed on San Nicolas Island off the coast of Southern California. The gray panel in the middle of the photo is the frame for the 449-MHz wind profiler coaxial–colinear phased array radar antenna. The octagonal enclosures house the acoustic antennas that are part of the RASS for temperature profiling. The wind profiler and RASS electronics are situated in the environmentally controlled trailer. The site also includes a 10-m meteorological tower (not shown) and a GPS receiver for IWV estimates.

TABLE 8. Locations for the four AROs being installed for the HMT-Legacy project. All are installed by ESRL.

Location	Station ID	Lat (°)	Lon (°)	Elev (m)	Installation date
McKinleyville, CA	ACV	40.972	−124.110	58	TBD
Bodega Bay, CA	BBY	38.319	−123.073	16	21 Mar 2013
Point Sur, CA	PTS	36.304	−121.888	13	TBD
Goleta, CA	GLA	34.429	−119.847	3	TBD

5. Examples of integrated observational and model forecast display products

Once the raw observations and model forecasts associated with the HMT-Legacy project are acquired and ingested, value-added data displays are produced in near-real time (www.esrl.noaa.gov/psd/data/obs/). Figure 10 illustrates a multipanel display of the snow-level product derived from 6 of the 10 snow-level radars stretching from Northern California to the south-central Sierra (see Fig. 3). This information is of primary importance to river forecasters to verify the snow levels predicted by numerical weather prediction models. In addition to providing information on the snow level, the snow-level radar network provides detail on the timing of precipitation and the depth (up to the radar's maximum range and subject to the radar's minimum sensitivity) of the precipitating cloud layer. For example, in the left-hand side of Fig. 10 the network depicts the time lag required for the onset of a storm's precipitation to proceed from north to south as the storm progresses down the coast of California.

Figure 11 shows an example of the water vapor flux tool display derived from a prototype ARO deployed in Sonoma County, California, as part of the HMT 2008/09 field season. This display, developed jointly by operational weather forecasters and HMT research scientists, combines observations with numerical weather prediction output to help monitor and forecast the forcings associated with landfalling ARs. Weather forecasters and other end users can use this tool to verify how well the HMT weather forecast model is portraying the AR conditions and the resulting precipitation. In the near future, the tool will include operational Rapid Refresh model output. HMT research is also being conducted to determine how far inland atmospheric rivers impact precipitation, runoff, and the potential for flooding.

The snow-level radar and water vapor flux tool displays have received positive feedback from NWS and the U.S. Army Corps of Engineers (ACE). Both agencies have noted that these products have increased their situational awareness of storm impacts.
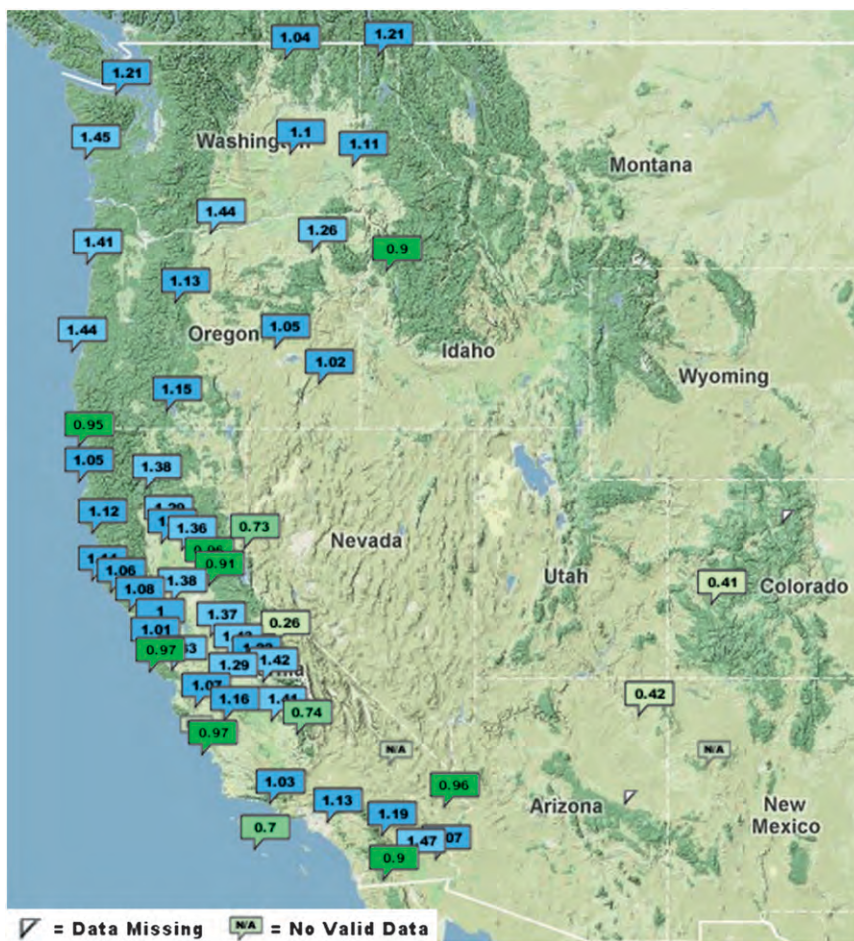
every 3 h using the GFS ensemble. A subset of forecast fields produced by the model is also publicly available (http://laps.noaa.gov/hmt/hmt.html).

To provide hourly model forecasts for the water vapor flux tool (see section 5), a separate WRF 3-km grid spacing (10-km grid spacing prior to 2013) model run is initialized every hour using LAPS. LAPS analyses are produced over the same West Coast domain and with the same horizontal grid spacing as the model. By reproducing the analysis every hour, the latest observations, both operational and experimental, are included for the next forecast cycle (Jian et al. 2003). The physics packages used in the model include the Thompson microphysics scheme (Thompson et al. 2004) and the nonlocal mixing Yonsei University (YSU) planetary boundary layer scheme (Noh et al. 2003). These schemes were chosen based on 5 years of experience gained in running the WRF model over the western United States for HMT (Jankov et al. 2007, 2009, 2011; Yuan et al. 2008, 2009). The analysis production starts 20 min after the hour in order to allow the latest data collected during the previous hour to arrive. The updated analysis grid is available approximately 45 min after the top of the hour. This new LAPS analysis is used to initialize the model, which then produces a 12-h forecast. The forecast, along with hourly output, is available approximately 2 h after the observations are collected. Gridpoint data extraction necessary for the water vapor flux tool is done almost instantaneously. The model output displayed on the right side of the flux tool (see section 5) is the 3-h forecast available from each successive hourly model run.

FIG. 9. Example of the Google Maps display of HMT-Legacy project integrated water vapor observations. This display system is publicly available (http://www.esrl.noaa.gov/psd/data/obs/ sitemap/psdmapdata/).

For example, Arthur Henkel, the development and operations hydrologist at the CNRFC, has said that the snow-level measurements generated by HMT have ''changed the way we do business with respect to snow-level forecasting.'' In another case, Larry Schick, meteorologist with the ACE office in Seattle, used the water flux display from an ARO deployed on the Washington coast, as part of the Howard A. Hanson Dam (HHD) flood risk mitigation project (White et al. 2012), to help make significant water management decisions during a series of storms that impacted western Washington in January 2012. He stated, ''Yesterday, I used the new coastal radar and ARO in tandem to refine the forecast and give our dam regulator engineers critical forecast information... Of course, I was monitoring local WFO Seattle NWS forecasts and Northwest River Forecast Center as well and they were right on, but the ARO does allow a strong confirmation for

making these rapidly changing but important dam operational decisions.'' White et al. (2012) also includes specific examples of and statistics on how the ARO observations were used in daily forecast operations during the HHD flood risk mitigation project.

6. Decision support tools

An important step in impacting forecast operations and end-user decisions is to develop decision support tools (DSTs) tailored to their needs, based on state-of-the-art knowledge and near-real-time data provided by this new observing and modeling system. An important component of this project's DST development is the role of atmospheric rivers in creating the heavy precipitation that can lead to flooding or to beneficial water supply (Dettinger et al. 2011). Based on HMT research, clearly defined criteria have now been established that identify
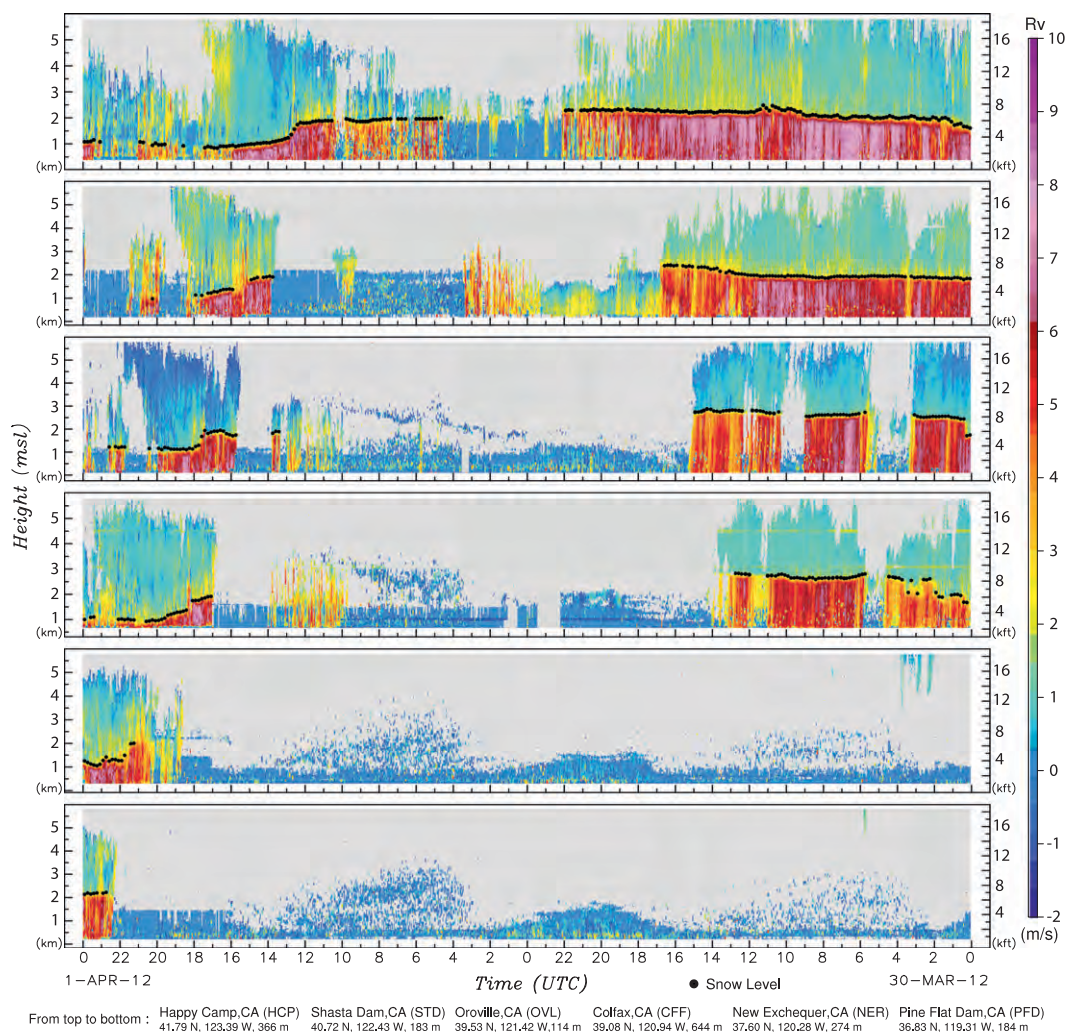
FIG.10. Time–height sections of Doppler vertical velocity and snow level measured by six snow-level radars deployed along the Sierra and in Northern California (from north to south; see Fig. 3). In precipitation, the Doppler vertical velocity (m s^{-1}; color contours) is closely related to the fall velocity of the hydrometeors. The altitude of the snow level is indicated by the black dots. The time series covers 48 h from 0000 UTC 30 Mar 2012 to 0000 UTC 1 Apr 2012. Time proceeds from right to left along the *x* axes.

when an AR is about to strike (e.g., Fig. 11). The location at landfall and intensity of ARs are also critical, and both of these parameters can now be monitored with the newly installed observing network. Numerical model forecast–based tools have been developed to better predict these events out to several days. For example, there is now an automated AR detection tool (Wick et al. 2013; http://www.esrl.noaa.gov/psd/psd2/coastal/satres/data/html/ar_detect_gfs_new.php) applied to the NWS operational Global Forecast System produced by NCEP.

An example of this advanced warning capability occurred in December 2010 when a major AR struck Southern California. Because of previous wild fire scars

on the mountains of Southern California, it was recognized that any heavy rainfall event could lead to large debris flows. A training session provided by one of the authors to all western region offices of the NWS just a few weeks earlier highlighted the importance and recognition of ARs. The positive impact of this training was demonstrated by forecasters having the confidence to alert state and local emergency management to the potential threat several days in advance. In fact, up to 48 h before 15–20 in. of rain fell in the San Bernardino Mountains of Southern California, forecasters were predicting up to 20 in. of rain to fall and warning of major debris flows, which allowed for earlier warnings and preparations. Over $60 million (U.S. dollars) in
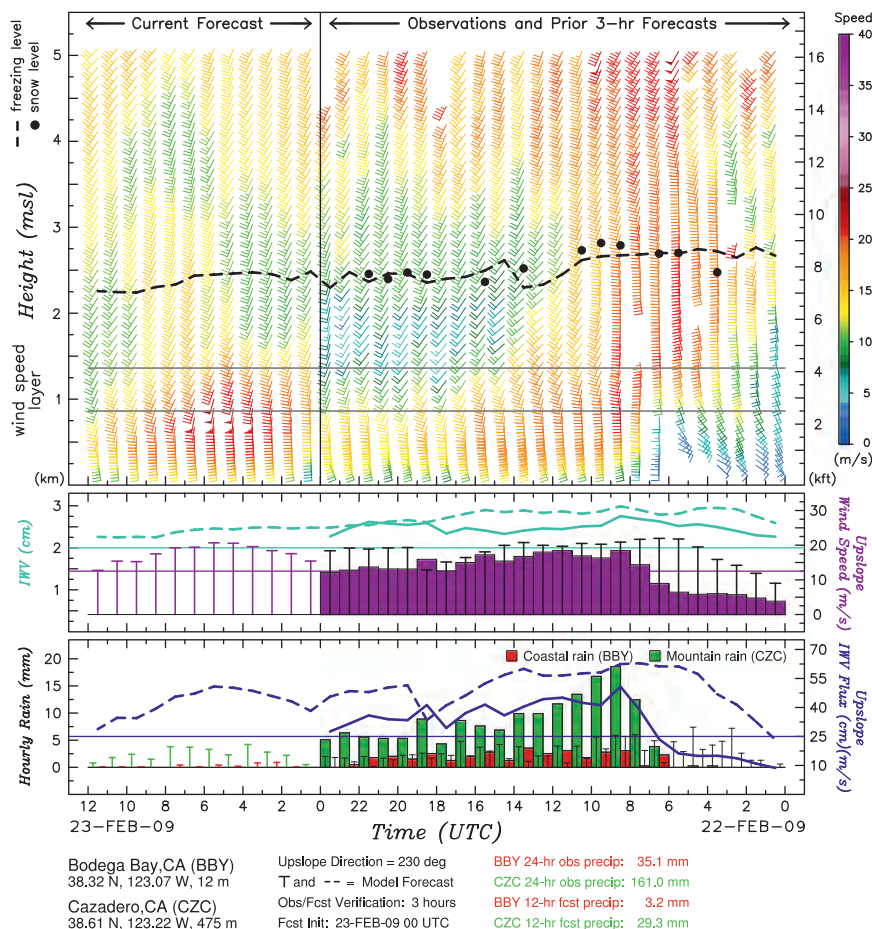
FIG. 11. Example from 22 to 23 Feb 2009 of the AR water vapor flux tool applied to sites in Northern California. (top) Wind profiler hourly averaged observations of the snow level (bold dots) and retrospective hourly HMT model forecasts of the freezing level (dashed line) at 3-h verification time along with time–height section of hourly averaged wind profiles (flags = $25\,\mathrm{m\,s^{-1}}$; barbs = $5\,\mathrm{m\,s^{-1}}$; half-barbs = $2.5\,\mathrm{m\,s^{-1}}$; wind speed color coded), observed by the ARO at Bodega Bay. (middle) Time series of hourly averaged upslope flow ($\mathrm{m\,s^{-1}}$; from 200°) observed (histogram) and predicted (T posts) in the layer between 750 and 1250 m MSL (bounded by the dashed lines in the top panel), and IWV (cm) observed (solid line) and predicted (dashed line) by the HMT forecast model. (bottom) Time series of hourly averaged IWV flux ($\mathrm{m\,s^{-1}\,cm}$) observed (solid line) and predicted (dashed line) by the HMT forecast model and hourly rainfall histogram from Bodega Bay (mm; red) and Cazadero (mm; green) in the coastal mountains. Time moves from right to left along the x axis. The current time is indicated by the vertical line in the top panel. Data plotted to the left of this line in each panel show the current HMT model forecast only (i.e., no observations), whereas data plotted to the right of the line in each panel are a combination of observations and model output. Minimum thresholds of upslope flow, IWV, and IWV flux for the potential occurrence of heavy rain ($>10\,\mathrm{mm\,h^{-1}}$) in atmospheric river conditions defined by Neiman et al. (2009) are indicated by the thin horizontal lines in the middle and bottom panels.

damages were reported in San Bernardino County from flash flooding and landslides. Some major cities in Southern California received over 50% of their average annual rainfall in just 7 days. Major flooding occurred along the Santa Margarita, San Diego, and Mojave Rivers.

A new direction in the DST realm is the development of performance measures for predictions that relate more effectively to the key conditions associated with ARs and extreme precipitation. Both Ralph et al. (2010) and White et al. (2010) describe new performance measures for forecast variables related to flooding, and

these measures are now available for testing and implementation. Another tool that is now available is a scaling for extreme rainfall (Ralph and Dettinger 2012) that is more intuitive to nonspecialists and that is not sensitive to changes in climate. This scaling is simply four "rainfall categories" (R-Cats) based on 3-day-total rainfall, and these R-Cats can be applied to observations or predictions. R-Cat 4 (>500 mm) is the most extreme rainfall category, and California is the only state outside of the southeastern United States, where the impacts of tropical storms and hurricanes are most prevalent, that has experienced R-Cat 4 events during the period 1950–2008.

7. Summary and future work

a. Summary

Some of the winter storms that are responsible for the bulk of California's water supply throughout the year are also responsible for generating destructive floods that result in the loss of lives and property. In California, as for the nation as a whole, floods produce more annual property damage, on average, than any other type of natural disaster. Recently, a U.S. Geological Survey Multi Hazards Demonstration Project called ARkStorm (for atmospheric river 1000; Porter et al. 2011) studied the impacts of a scientifically plausible epic storm hitting California and found that such an event could result in $725 billion in losses. Furthermore, this project estimated that improved forecasting and warnings could reduce losses by tens of billions of dollars.

To provide forecasters, water managers, and the general public with the atmospheric and surface conditions that lead to heavy precipitation and flooding, CA-DWR is working with HMT-West and partners to install an unprecedented observing system across the state. The system consists of four synergistic observing networks that monitor the atmospheric and terrestrial conditions that can lead to dangerous floods and debris flows: 43 soil moisture, soil temperature, and surface meteorology stations; 36 GPS-Met integrated water vapor–observing sites; 10 snow-level radar and surface meteorology stations; and four coastal atmospheric river observatories. Through data assimilation, observations from these networks will provide improved initialization fields to drive weather forecast models. Long-term operation of the observing system will provide data to interpret how California's climate is changing and whether adaptation through new water management strategies will be required.

b. Future work

To maximize the impact of the HMT-Legacy project, future work will include developing training modules to increase the usage of the observations, models, and decision support tools within the NWS and also with water managers in the U.S. Army Corps of Engineers, U.S. Bureau of Reclamation, and local water agencies throughout California. ESRL is currently working on a new agreement with CA-DWR to 1) implement a plan to sustain the HMT-Legacy observations, 2) develop new decision support tools, and 3) optimize observing network expansion to provide watershed-scale information on extreme events. The last element will employ data denial experiments to help quantify the benefit of the additional observations on numerical weather forecasts.

In the spring of 2013, the HMT will begin a pilot project in North Carolina. This HMT–Southeast pilot study (HMT–SEPS) will have a warm-season precipitation focus, but ESRL's observing assets will be available year-round. In 2014, after the launch of the Global Precipitation Measurement mission's core satellite, NASA will bring a number of observing assets to bear on HMT–Southeast, including scanning radars, disdrometers, and rain gauges.

The HMT-Legacy project already has generated action on at least two fronts. First, UNAVCO and NOAA have expanded the GPS water vapor monitoring network by 25 stations in the western United States, including 13 in Oregon and Washington combined. This expansion will help with tracking the inland penetration of ARs throughout the Pacific Northwest. Second, the Western States Water Council (http://www.westernstateswater.org/) adopted Position 322 (Western States Water Council 2011) in July 2011, which includes the following statement: "Be it further resolved, that the Western States Water Council supports development of an improved observing system for Western extreme precipitation events, to aid in monitoring, prediction, and climate trend analysis associated with extreme weather events." At the time of this publication, an implementation plan for this western states–wide observing system was being developed at the request of the Western Governors' Association (http://www.westgov.org/).

REFERENCES

Albers, S., J. McGinley, D. Birkenheuer, and J. Smart, 1996: The Local Analysis and Prediction System (LAPS): Analyses of clouds, precipitation, and temperature. *Wea. Forecasting,* **11,** 273–287.

Battan, L. J., 1959: *Radar Meteorology.* University of Chicago Press, 161 pp.

Bevis, M., S. Businger, T. A. Herring, C. Rocken, R. A. Anthes, and R. H. Ware, 1992: GPS meteorology: Remote sensing of the atmospheric water vapor using the global positioning system. *J. Geophys. Res.,* **97** (D14), 15 787–15 801.

Carter, D. A., K. S. Gage, W. L. Ecklund, W. M. Angevine, P. E. Johnston, A. C. Riddle, J. Wilson, and C. R. Williams, 1995: Developments in UHF lower tropospheric wind profiling at NOAA's Aeronomy Laboratory. *Radio Sci.,* **30,** 977–1001.

Cayan, D. R., E. P. Maurer, M. D. Dettinger, M. Tyree, and K. Hayhoe, 2008: Climate change scenarios for the California region. *Climatic Change,* **87** (Suppl.), 21–42, doi:10.1007/s10584-007-9377-6.

——, T. Das, D. W. Pierce, T. P. Barnett, M. Tyree, and A. Gershunov, 2010: Future dryness in the southwest U.S. and the hydrology of the early 21st century drought. *Proc. Natl. Acad. Sci. USA,* **107,** 21 271–21 276.

——, and Coauthors, 2013: Future climate: Projected average. *Assessment of Climate Change in the Southwest United States: A Report Prepared for the National Climate Assessment,* G. Garfin et al., Eds., Island Press, 101–125.

Das, T., M. Dettinger, D. Cayan, and H. Hidalgo, 2011: Potential increase in floods in California's Sierra Nevada under future climate projections. *Climatic Change,* **109,** 71–94.

Dettinger, M. D., 2011: Climate change, atmospheric rivers, and floods in California—A multimodel analysis of storm frequency and magnitude changes. *J. Amer. Water Resour. Assoc.,* **47,** 514–523.

——, F. M. Ralph, T. Das, P. J. Neiman, and D. R. Cayan, 2011: Atmospheric rivers, floods and the water resources of California. *Water,* **3,** 445–478.

Duan, J., and Coauthors, 1996: GPS meteorology: Direct estimation of the absolute value of precipitable water. *J. Appl. Meteor.,* **35,** 830–838.

Dunne, T., and R. D. Black, 1970: An experimental investigation of runoff production in permeable soil. *Water Resour. Res.,* **6,** 478–490.

Guan, B., N. P. Molotch, D. E. Waliser, E. J. Fetzer, and P. J. Neiman, 2010: Extreme snowfall events linked to atmospheric rivers and surface air temperature via satellite measurements. *Geophys. Res. Lett.,* **37,** L20401, doi:10.1029/2010GL044696.

Gutman, S. I., S. R. Sahm, S. G. Benjamin, B. E. Schwartz, K. L. Holub, J. Q. Stewart, and T. L. Smith, 2004: Rapid retrieval and assimilation of ground based GPS precipitable water observations at the NOAA Forecast Systems Laboratory: Impact on weather forecasts. *J. Meteor. Soc. Japan,* **82,** 351–360.

Jankov, I., P. J. Schultz, C. J. Anderson, and S. E. Koch, 2007: The impact of different physical parameterizations and their interactions on cold season QPF in the American River basin. *J. Hydrometeor.,* **8,** 1141–1151.

——, J.-W. Bao, P. J. Neiman, P. J. Schultz, H. Yuan, and A. B. White, 2009: Evaluation and comparison of microphysical algorithms in WRF-ARW model simulations of atmospheric river events affecting the California coast. *J. Hydrometeor.,* **10,** 847–870.

——, and Coauthors, 2011: An evaluation of five WRF-ARW microphysics schemes using synthetic GOES imagery for an atmospheric river event affecting the California coast. *J. Hydrometeor.,* **12,** 618–633.

Jian, G.-J., S.-L. Shieh, and J. A. McGinley, 2003: Precipitation simulation associated with Typhoon Sinlaku (2002) in the Taiwan area using the LAPS diabatic initialization for MM5. *Terr. Atmos. Ocean. Sci.,* **14,** 261–288.

Johnston, P. E., D. A. Carter, D. M. Costa, J. R. Jordan, and A. B. White, 2012: A new FM-CW radar for precipitation and boundary-layer science. *Extended Abstracts, 16th Int. Symp. for the Advancement of Boundary-Layer Remote Sensing,* Boulder, CO, Cooperative Institute for Research in Environmental Sciences and NOAA Earth System Research Laboratory, 306–309.

Jordan, J. R., R. J. Lataitis, and D. M. Costa, 1998: Motion compensation for buoy mounted wind profiling radars. *Proc. Fourth Int. Symp. on Tropospheric Profiling: Needs and Technologies*, Snowmass, CO, University of Colorado, 155–157.

Jorgensen, D. P., M. N. Hanshaw, K. M. Schmidt, J. L. Laber, D. M. Staley, J. W. Kean, and P. J. Restrepo, 2011: Value of a dual-polarized gap-filling radar in support of southern California post-fire debris-flow warnings. *J. Hydrometeor.,* **12,** 1581–1595.

Kingsmill, D. E., A. B. White, P. J. Neiman, and F. M. Ralph, 2006: Synoptic and topographic variability of northern California precipitation characteristics in landfalling winter storms observed during CALJET. *Mon. Wea. Rev.,* **134,** 2072–2094.

Knowles, N., and D. Cayan, 2004: Elevational dependence of projected hydrologic changes in the San Francisco estuary and watershed. *Climatic Change,* **62,** 319–336.

Lavers, D. A., R. P. Allan, E. F. Wood, G. Villarini, D. J. Brayshaw, and A. J. Wade, 2011: Winter floods in Britain are connected to atmospheric rivers. *Geophys. Res. Lett.,* **38,** L23803, doi:10.1029/2011GL049783.

Martner, B. E., S. E. Yuter, A. B. White, S. Y. Matrosov, D. E. Kingsmill, and F. M. Ralph, 2008: Raindrop size distributions and rain characteristics in California coastal rainfall for periods with and without a radar brightband. *J. Hydrometeor.,* **9,** 408–425.

Matrosov, S. Y., D. E. Kingsmill, B. E. Martner, and F. M. Ralph, 2005: The utility of X-band polarimetric radar for quantitative estimates of rainfall parameters. *J. Hydrometeor.,* **6,** 248–262.

Moore, B. J., P. J. Neiman, F. M. Ralph, and F. E. Barthold, 2012: Physical processes associated with heavy flooding rainfall in Nashville, Tennessee, and vicinity during 1–2 May 2010: The role of an atmospheric river and mesoscale convective systems. *Mon. Wea. Rev.,* **140,** 358–378.

Moran, K. P., and R. G. Strauch, 1994: The accuracy of RASS temperature measurements corrected for vertical air motion. *J. Atmos. Oceanic Technol.,* **11,** 995–1001.

Morss, R. E., and F. M. Ralph, 2007: Use of information by National Weather Service forecasters and emergency managers during CALJET and PACJET-2001. *Wea. Forecasting,* **22,** 539–555.

Neiman, P. J., F. M. Ralph, A. B. White, D. E. Kingsmill, and P. O. G. Persson, 2002: The statistical relationship between upslope flow and rainfall in California's coastal mountains: Observations during CALJET. *Mon. Wea. Rev.,* **130,** 1468–1492.

——, B. E. Martner, A. B. White, G. A. Wick, F. M. Ralph, and D. E. Kingsmill, 2005: Wintertime nonbrightband rain in

California and Oregon during CALJET and PACJET: Geographic, interannual, and synoptic variability. *Mon. Wea. Rev.,* **133,** 1199–1223.

——, F. M. Ralph, G. A. Wick, J. D. Lundquist, and M. D. Dettinger, 2008: Meteorological characteristics and overland precipitation impacts of atmospheric rivers affecting the West Coast of North America based on eight years of SSM/I satellite observations. *J. Hydrometeor.,* **9,** 22–47.

——, A. B. White, F. M. Ralph, D. J. Gottas, and S. I. Gutman, 2009: A water vapour flux tool for precipitation forecasting. *Proc. Inst. Civ. Eng.—Water Manage.,* **162,** 83–94.

Noh, Y., W. G. Cheon, S.-Y. Hong, and S. Raasch, 2003: Improvement of the K-profile model for the planetary boundary layer based on large eddy simulation data. *Bound.-Layer Meteor.,* **107,** 401–427.

Peixoto, J. P., and A. H. Oort, 1992: *Physics of Climate.* American Institute of Physics, 520 pp.

Porter, K., and Coauthors, 2011: Overview of the ARkStorm scenario. U.S. Geological Survey Open-File Rep. 2010–1312, 183 pp. [Available online at http://pubs.usgs.gov/of/2010/1312/.]

Prigent, C., J.-P. Wigneron, W. B. Rossow, and J. R. Pardo-Carrion, 2000: Frequency and angular variations of land surface microwave emissivities: Can we estimate SSM/T and AMSU emissivities from SSM/I emissivities? *IEEE Trans. Geosci. Remote Sens.,* **38,** 2373–2386.

Ralph, F. M., and M. D. Dettinger, 2012: Historical and national perspectives on extreme West Coast precipitation associated with atmospheric rivers during December 2010. *Bull. Amer. Meteor. Soc.,* **93,** 783–790.

——, P. J. Neiman, D. E. Kingsmill, P. O. G. Persson, A. B. White, E. T. Strem, E. D. Andrews, and R. C. Antweiler, 2003: The impact of a prominent rain shadow on flooding in California's Santa Cruz Mountains: A CALJET case study and sensitivity to the ENSO cycle. *J. Hydrometeor.,* **4,** 1243–1264.

——, ——, and G. A. Wick, 2004: Satellite and CALJET aircraft observations of atmospheric rivers over the eastern North Pacific Ocean during the winter of 1997/98. *Mon. Wea. Rev.,* **132,** 1721–1745.

——, and Coauthors, 2005: Improving short-term (0–48 h) cool-season quantitative precipitation forecasting: Recommendations from a USWRP workshop. *Bull. Amer. Meteor. Soc.,* **86,** 1619–1632.

——, P. J. Neiman, G. A. Wick, S. I. Gutman, M. D. Dettinger, C. R. Cayan, and A. B. White, 2006: Flooding on California's Russian River: Role of atmospheric rivers. *Geophys. Res. Lett.,* **33,** L13801, doi:10.1029/2006GL026689.

——, E. Sukovich, D. Reynolds, M. Dettinger, S. Weagle, W. Clark, and P. J. Neiman, 2010: Assessment of extreme quantitative precipitation forecasts and development of regional extreme event thresholds using data from HMT-2006 and COOP observers. *J. Hydrometeor.,* **11,** 1286–1304.

Skamarock, W. C., and J. B. Klemp, 2008: A time-split nonhydrostatic atmospheric model for research and NWP applications. *J. Comput. Phys.,* **227,** 3465–3485.

Thompson, G., R. M. Rasmussen, and K. Manning, 2004: Explicit forecasts of winter precipitation using an improved bulk microphysics scheme. *Mon. Wea. Rev.,* **132,** 519–542.

Toth, Z., S. Albers, and Y. Xie, 2012: Analysis of fine-scale weather phenomena. *Bull. Amer. Meteor. Soc.,* **93,** ES35–ES38.

Western States Water Council, 2011: Resolution of the Western States Water Council supporting federal research and development of updated hydroclimate guidance for extreme meteorological events. Policy Statement 332, 2 pp. [Available online at http://www.westernstateswater.org/policies-2/.]

White, A. B., J. R. Jordan, B. E. Martner, F. M. Ralph, and B. W. Bartram, 2000: Extending the dynamic range of an S-band radar for cloud and precipitation studies. *J. Atmos. Oceanic Technol.,* **17,** 1226–1234.

——, D. J. Gottas, E. T. Strem, F. M. Ralph, and P. J. Neiman, 2002: An automated brightband height detection algorithm for use with Doppler radar spectral moments. *J. Atmos. Oceanic Technol.,* **19,** 687–697.

——, P. J. Neiman, F. M. Ralph, D. E. Kingsmill, and P. O. G. Persson, 2003: Coastal orographic rainfall processes observed by radar during the California Land-Falling Jets Experiment. *J. Hydrometeor.,* **4,** 264–282.

——, F. M. Ralph, P. J. Neiman, D. J. Gottas, and S. I. Gutman, 2009: The NOAA coastal atmospheric river observatory. Preprints, *34th Conf. on Radar Meteorology,* Williamsburg, VA, Amer. Meteor. Soc., 10B.4. [Available online at http://ams.confex.com/ams/pdfpapers/155601.pdf.]

——, D. J. Gottas, A. F. Henkel, P. J. Neiman, F. M. Ralph, and S. I. Gutman, 2010: Developing a performance measure for snow-level forecasts. *J. Hydrometeor.,* **11,** 739–753.

——, and Coauthors, 2012: NOAA's rapid response to the Howard A. Hanson Dam flood risk management crisis. *Bull. Amer. Meteor. Soc.,* **93,** 189–207.

Wick, G. A., P. J. Neiman, and F. M. Ralph, 2013: Description and validation of an automated objective technique for identification and characterization of the integrated water vapor signature of atmospheric rivers. *IEEE Trans. Geosci. Remote Sens.,* **51,** 2166–2176.

Yuan, H., J. A. McGinley, P. J. Schultz, C. J. Anderson, and C. Lu, 2008: Short-range precipitation forecasts from time-lagged multimodel ensembles during the HMT-West-2006 campaign. *J. Hydrometeor.,* **9,** 477–491.

——, C. Lu, J. A. McGinley, P. J. Schultz, B. D. Jamison, L. Wharton, and C. J. Anderson, 2009: Evaluation of short-range quantitative precipitation forecasts from a time-lagged multimodel ensemble. *Wea. Forecasting,* **24,** 18–38.

Zamora, R. J., F. M. Ralph, E. Clark, and T. Schneider, 2011: The NOAA hydrometeorology testbed soil moisture observing networks: Design, instrumentation, and preliminary results. *J. Atmos. Oceanic Technol.,* **28,** 1129–1140.

Zhu, Y., and R. E. Newell, 1998: A proposed algorithm for moisture fluxes from atmospheric rivers. *Mon. Wea. Rev.,* **126,** 725–735.